Anisotropy in ordered sexithiophene thin films studied by angle-resolved photoemission using combined laser and synchrotron radiation

C. E. Heiner,[a] J. Dreyer, I. V. Hertel,[b] N. Koch,[c] H.-H. Ritze, W. Widdra,[d] and B. Winter
Max-Born-Institut für Nichtlineare Optik and Kurzzeitspektroskopie, Max-Born-Str. 2A, D-12489 Berlin, Germany

(Received 15 February 2005; accepted 14 July 2005; published online 22 August 2005)

We present angle-resolved photoemission (PE) spectra of ordered multilayer sexithiophene (6T) films, 200 nm thick, grown on a Au(110) single crystal. However, the measurement of sharp and nonshifted PE spectral features from the low-conducting organic material is only possible if the positive surface charge, generated in the PE process, is fully compensated. We have accomplished this by simultaneous laser irradiation. On the basis of the resulting data we found that for these thick films the 6T molecules are preferentially oriented with their long axes nearly normal to the surface. © *2005 American Institute of Physics*. [DOI: 10.1063/1.2034105]

In recent years systems of π-conjugated organic materials, such as oligothiophenes, have been intensively studied for their technological application potential.[1–3] The ability to control the film's properties requires an understanding of the fundamental electronic and physical structure. In fact, the system's physical properties (including growth) greatly depend on the interactions between the individual organic molecules, and hence specifically on their relative orientation within the film. For instance, orientational disorder of molecules in the sexithiophene (6T) crystalline herringbone lattice were shown to strongly affect the crystal's optical and electronic properties.[4] Long-range ordered multilayers may be grown on crystalline surfaces, i.e., on an oriented seed monolayer arising from the specific surface bonding mechanism, which varies depending on substrate. Specifically, the 6T overlayer on Au(110) has been shown to act as a template for planar and well-ordered growth of at least five molecular layers.[5]

Films were grown on a (1×2)-Au(110) single-crystal surface. 6T (Syncom BV) was evaporated from a Knudsen cell (250 °C yielding ≈0.02 nm/s deposition rate), with the crystal kept at room temperature. The base pressure of the preparation chamber was 2×10^{-10} mbar. The gold substrate was cleaned by repeated cycles of argon ion sputtering and annealing, resulting in a sharp (1×2) low-electron energy diffraction (LEED) pattern of the clean reconstructed gold surface. At nearly one monolayer 6T coverage a (quasicommensurate) slightly streaked (1×3) LEED pattern was observed; this was attributed to the widening of the missing row [001] resulting in the long, asymmetric 6T molecules preferred nucleation along the $[1\bar{1}0]$ direction.[5] Continual deposition of 6T eventually led to islands, which still possessed the same preferred orientation within the thicker film. Atomic force microscopic (AFM) images of such films exhibited (interconnected) column-type structures. A quite similar film morphology, though for considerably smaller thickness, has been reported for 6T grown on potassium acid phthalate (KAP) [001] substrates.[6]

The PE experiments were performed at the undulator beamline of the Max-Born-Institut (U125 SGM) at the Berlin Electron Synchrotron Facility, BESSY. Photoelectrons were detected by a hemispherical electron energy analyzer (EA 125, Omicron) within ±1° sample take-off, set to an energy resolution of 150 meV. Angle-resolved PE was measured for grazing light incidence ($\Psi_i=83°$) at varied electron emission angle ($0°<\Theta_e<20°$). The PE spectra presented here were collected during both BESSY multi and single bunch operation, corresponding to interpulse spacing of the synchrotron radiation (SR) of 2 ns(500 MHz) and 800 ns(1.25 MHz), respectively. In order to compensate for sample charging we have applied simultaneous laser irradiation (LR), with the laser pulses being synchronized to the synchrotron pulses: either 400 nm from a Ti:sapphire laser (83 MHz repetition, 200 fs width, ≈500 mW at second harmonic), used for multibunch, or 532 nm from a $Nd:YVO_4$ laser (pulse-picked to 1.25 MHz, 14 ps pulse width, ≈200 nJ pulse energy), used for the single bunch. Both laser wavelengths were equally suited to remove charging, and equally sharp and well-resolved spectra were measured. Foci at the sample were about 200×800 μm^2 (SR) and 1 mm diameter (LR).

Figure 1 presents PE spectra for 200 nm 6T deposited on Au(110), which contrasts the effect of the laser on (bottom) versus laser off (top). For this particular thickness the gold substrate signal is fully suppressed and hence features in the PE spectra, and later angular dependencies, can be unequivocally attributed to the organic film only. The spectra were consecutively measured at grazing incidence in normal emission, for 50 eV photon energy in multi bunch, and applying 400 nm laser pulses (100 mW). The curves are normalized to the (nearly identical) background signal near 25 eV binding energy (BE), and energies are given with respect to the Fermi energy.

Only upon laser irradiation do the peaks derived from 6T molecular orbitals appear at their true electron binding energies (as determined through a coverage series), and obviously the overall spectral resolution is greatly improved. The effect is most noticeable for feature A, where we observe the

[a]Author to whom correspondence should be addressed; present address: Fritz-Haber-Institut der Max-Planck-Gesellschaft, D-14195 Berlin, Germany; electronic mail: heiner@fhi-berlin.mpg.de
[b]Also at: Fachbereich Physik, Freie Universität Berlin, D-14195 Berlin, Germany.
[c]Humboldt Universität zu Berlin, Institut für Physik, Berlin D-12489 Berlin, Germany.
[d]Present address: Martin-Luther-Universität Halle-Wittenberg, D-06099 Halle, Germany.

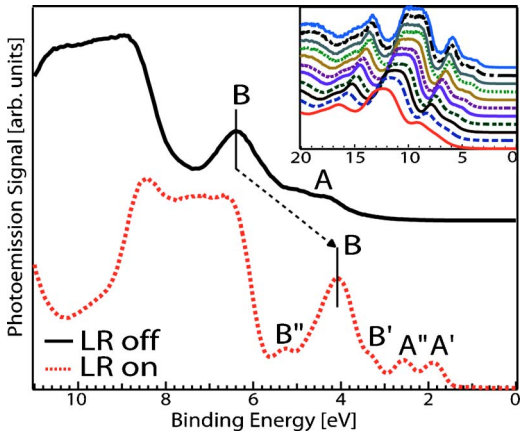

FIG. 1. (Color online) Photoemission spectra of a 200 nm 6T/Au(110) film, measured at 50 eV photon energy, with (bottom) and without (top) the addition of 400 nm LR (Ti:sapphire, 100 mW). Inset: PE spectra, without LR, as a function of the SR flux displayed on an extended energy scale. The spectra are vertically shifted for clarity. From bottom to top the flux has been reduced gradually, from maximum (new fill) to 1/100 of maximum.

emergence of two distinctive peaks, at 1.85 eV (A′) and 2.55 eV (A″) BE. These peaks represent the two highest occupied molecular orbitals, HOMO and HOMO-1, respectively. Also, the localized π band region (B) is shifted by 2.1 eV to its true value at 4.1 eV BE, and again is considerably sharpened for the laser-excited sample as documented by two defined shoulders, B′ at 3.3 eV and B″ at 5.25 eV BE (derived from delocalized π-orbitals; B′ corresponds to HOMO-2).

Peak shift and broadening can be attributed to sample charging. The former is a direct consequence of the photoelectrons being slowed down by the accumulated positive surface charge. The broadening is suggested to correlate with the rough surface (due to island growth as inferred from AFM measurements), since regions of larger thickness will tend to be more charged. Two mechanisms provide for charge neutralization: internal photoemission and the formation of charge carriers after photoexcitation of organic molecules.[7] The rigid spectral shift scales with the actual synchrotron light intensity used. This is illustrated in the inset of Fig. 1, showing a series of valence band spectra from 200 nm 6T/Au(110) as a function of synchrotron photon flux (achieved by detuning the undulator gap), using 50 eV photons in the absence of additional laser pulses. Charging shifts range from 1.75 to 5.0 eV; i.e., even for the most moderate excitation conditions spectral shifts occur (this equally applies for single and multi bunch), and must be compensated. Angle-resolved PE spectra presented in the following have been obtained at conditions where charging was fully compensated.

Figure 2 displays the angle-resolved PE spectra for various geometrical situations, obtained at 50 eV photon energy in single bunch operation using simultaneous LR of 532 nm($Nd:YVO_4$). The nomenclature for the experimental geometries are described by E (excitation) and D (detection), whose subscripts (x,y,z) refer to the direction of the SR polarization vector and the direction of photoelectron detection, respectively.[8] Note that for D_x (D_y) the velocity vector of the detected electrons lies in the xz (yz) plane. The emission angle, Θ_e, defines the angle between z-direction and this velocity vector. Spectra were measured in both normal emission (NE), $\Theta_e=0$, where photoelectrons are detected along the z-axis, and off NE, $\Theta_e>0$, where detection is in the x or y plane (i.e., xz or yz) as marked. For example, when the incident SR is polarized in the x direction, and the emitted electrons are detected in the xz plane, the corresponding geometry would be E_xD_x. This experimental geometry is sketched as an inset in Fig. 2. The coordinate system is defined as x and y being the direction along the substrate's crystallographic axes $[1\bar{1}0]$ and [001]. All spectra shown are measured in NE unless otherwise stated.

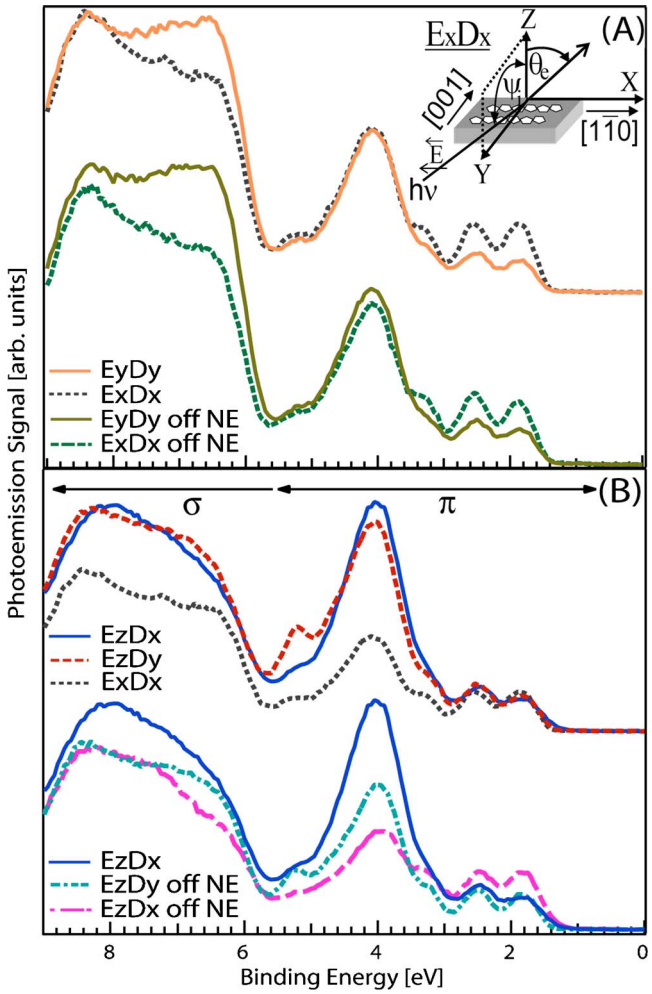

FIG. 2. (Color online) Photoemission spectra from 200 nm 6T/Au(110) obtained in several experimental geometries for 50 eV photon energy with an additional LR of 532 nm($\approx$50 mW). (A) and (B) geometry: $E\|[1\bar{1}0]$ vs $E\perp[1\bar{1}0]$: normal emission (top); 20°-off NE (bottom). Inset: The E_xD_x experimental geometry and framework.

The spectra in Fig. 2(A) illustrate the differences of positioning the SR polarization vector parallel to the $[1\bar{1}0]$ (E_xD_x) or [001] (E_yD_y) directions. The top two spectra were obtained in NE, the bottom two for 20° off NE. For the pairs of spectra in Fig. 2(B), the SR polarization was kept constant in the z-direction. Within each pair, the spectra differ in the azimuth of the sample, thus providing detection either parallel to $(z-x)$ or cutting across $(z-y)$ the $[1\bar{1}0]$ axis, and again were measured in both NE (top) and 20° off NE (bottom). The dotted line in Fig. 2(B) reproduces the E_xD_x spectrum at normal emission for comparison. Again, all spectra were normalized to the background signal near 25 eV.

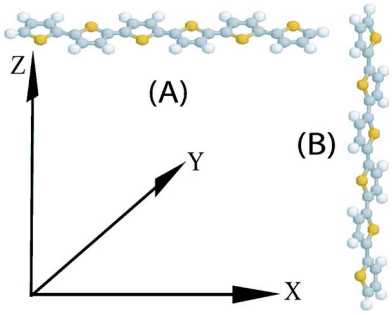

FIG. 3. (Color online) Two different orientations of a sexithiophene molecule relative to the gold substrate. The molecular planes are parallel to *xy* (A), nearly parallel to *yz* (B). The Cartesian frame is the same as in the inset of Fig. 2.

Typically, the signal in the π region of HOMO, HOMO-1, and HOMO-2 is $\approx$50% enhanced in the *x*-detection plane, regardless of Θ_e. A reversed effect, i.e., a stronger D_y signal, is seen in the spectra in Fig. 2(A) between the σ regime of 5.7 eV and 8.0 eV BE, and in the spectra in Fig. 2(B) at the shoulder at 5.3 eV BE. It is also clear that for $\Theta_e=0$ the experimental result for E_zD_x has to be the same as for E_zD_y, since in this case the electron's velocity vector remains the same despite the rotation of the sample's azimuths. Hence, one would expect almost identical spectra that we do, in fact, observe. The peak at 5.3 eV BE is the only exception, which is attributed to the fact that the E_z light polarization vector is not fully perpendicular to the crystal surface (otherwise the SR light would not reach the sample). However, the fact that all other features match ensures that this effect is negligible, especially in the crucial region of low BE π states.

The prominent azimuthal effects in the σ region and the localized π peak B cannot be discussed using simple selection rules due to the many, specifically for peak B six, near-degenerate orbitals. However, the low BE delocalized π orbitals, HOMO and HOMO-1, can be assigned decisively to the molecular orbitals with B_g and A_u, for C_{2h}, symmetry (planar 6T molecule). The symmetry selection rules are applied for different orientations of the molecules illustrated in Fig. 3. In Fig. 3(A) the molecular plane is parallel to the surface, and the long molecular axis is oriented along the *x*-direction; this situation applies for the first few layers.[5] In this case, NE is allowed for HOMO but forbidden for HOMO-1, which does not support the experimental data for these thicker films (HOMO and HOMO-1 show the same behavior). The problem persists, if the molecular plane is tilted by 90° and the long molecular axis remains unchanged.

Clearly for thicker films, we must consider another change in the 6T orientation, as outlined in Fig. 3(B). Here the molecules are "standing," i.e., their long axes are nearly vertical to the surface. A preferential "standing" orientation of the 6T molecules was found to occur on a Cu surface[9] and was also recently observed for 6T films of about 20 nm thickness on a Si substrate.[10] According to the C_{2h} selection rules, normal emission for both HOMO and HOMO-1 is forbidden for the E_yD_y geometry, and allowed for E_xD_x. The E_xD_x angular distribution of the emission from HOMO-1 is isotropic, while the signal from the HOMO orbital shows an anisotropic character (this is the change of the angular dependence of the emitted electron). It follows that for off-NE detection the HOMO signal decreases but the HOMO-1 remains constant. For a detection angle $\Theta_e=20°$ we expect that the HOMO signal is $\cos^2\Theta_e\approx0.88$ as large as the NE signal. This effect is in fact observed in Fig. 2(A), where the off NE HOMO signal slightly decreases relative to HOMO-1. Additionally, this agrees with the observed signal rise for E_zD_x off NE in the bottom of Fig. 2(B).

A weaker but nonvanishing emission from the highest two occupied orbitals in the E_yD_y geometries is observed which, under the strict orientation of Fig. 3(B), would be forbidden. This is not surprising given that in the crystal the molecules arrange in a herringbone packing, where the long molecular axes form an angle of $\sim$23° with the surface normal z;[11,12] this weakens the signal's Θ_e dependence. Additionally, in the herringbone structure two 6T molecules in the unit cell have an angle (τ) of 66° between molecular planes.[11] By assuming that half of the molecular planes are tilted from the *x* direction at +33°, and half at −33°, an optical anisotropy will still remain. Here the E_yD_y signal is about 0.42 times that of the E_xD_x. This agrees well with our experimental findings of $\approx$50% less signal for E_yD_y versus E_xD_x. Additionally, the presence of more than one 6T polymorph,[10] and the 83° light incidence component will result in a small fraction of other dipole transitions, which would otherwise be forbidden.

In summary, we have demonstrated that well-resolved photoemission spectra of relatively thick, well oriented sexithiophene films can only be measured in conjunction with laser irradiation. Using this approach, sharp angle-resolved PE spectra were obtained for 200 nm thick 6T films on Au(110). The application of symmetry selection rules allowed for the assessment of the molecular orientation from valence region emission, specifically the low BE π orbitals. Although for the first few molecular layers, the long molecular axis of sexithiophene is parallel to Au $[1\bar{1}0]$,[5] with increasing thickness a "skipjack" effect occurs, i.e., the angle between the long molecular axis and the surface increases. The observed pronounced anisotropy of the electron emission strongly suggests that in thick films (>200 nm) the molecules are in their preferred herringbone packing structure, with the crystallographic *c*-axis perpendicular to the substrate.

[1] G. Witte and C. Woell, J. Mater. Res. **19**, 1889 (2004).
[2] G. Horowitz, S. Romdhane, H. Bouchriha, P. Delannoy, J. L. Monge, F. Kouki, and P. Valat, Synth. Met. **90**, 187 (1997).
[3] H. Fujimoto, U. Nagashima, H. Inokuchi, K. Seki, Y. Cao, H. Nakahara, J. Nakayama, M. Hoshino, and K. Fukuda, J. Chem. Phys. **92**, 4077 (1990).
[4] F. Meinardi, M. Cerminara, S. Blumstengel, A. Sassella, A. Borghesi, and R. Tubino, Phys. Rev. B **67**, 184205 (2003).
[5] S. Prato, L. Floreano, D. Cvetko, V. De Renzi, A. Morgante, S. Modesti, F. Biscarini, R. Zamboni, and C. Taliani, J. Phys. Chem. B **103**, 7788 (1999).
[6] S. Tavazzi, G. Barbarella, A. Borghesi, F. Meinardi, A. Sassella, and R. Tubino, Synth. Met. **121**, 1419 (2001).
[7] N. Koch, D. Pop, R. L. Weber, N. Böwering, B. Winter, M. Wick, G. Leising, I. V. Hertel, and W. Braun, Thin Solid Films **391**, 81 (2001).
[8] G. Koller, F. P. Netzer, and M. G. Ramsey, Surf. Sci. **421**, 353 (1999).
[9] M. Kiguchi, G. Yoshikawa, and K. Saiki, J. Appl. Phys. **94**, 4866 (2003).
[10] J. Ivanco, J. R. Krenn, M. G. Ramsey, F. P. Netzer, T. Haber, R. Resel, A. Haase, B. Stadlober, and G. Jakopic, J. Appl. Phys. **96**, 2716 (2004).
[11] G. Horowitz, B. Bachet, A. Yassar, P. Lang, F. Demanze, J. L. Fave, and F. Garnier, Chem. Mater. **7**, 1337 (1995).
[12] J. C. Wittman, C. Straupe, S. Meyer, B. Lotz, P. Lang, G. Horowitz, and F. Garnier, Thin Solid Films **333**, 272 (1998).